Granular Turbulence in Two-Dimensions
— Microscale Reynolds Number and Final Condensed States —

Masaharu Isobe*
Graduate School of Engineering, Nagoya Institute of Technology, 466-8555, Japan.
(Dated: May 2, 2012)

Granular gases from the viewpoint of "two-dimensional turbulence" are investigated. In the quasi-elastic and thermodynamic limit, we obtained clear evidence for an enstrophy (square of vorticity) cascade and -3 exponent in the Kraichnan-Leith-Bachelor energy spectrum by performing large-scale ($N \sim 16.8$ million number of disks) event-driven molecular dynamics simulations. In these calculations, the enstrophy dissipation rate showed a strong relationship with the evolution of the exponent in the energy spectrum. The growth of the Reynolds number based on the microscale confirmed that the enstrophy cascade regime was that of fully developed turbulence. Moreover, a condensed state resembling Bose-Einstein condensation in decaying two-dimensional Navier-Stokes turbulence also appeared as the final attractor of the evolving granular gas in the long time limit.

PACS numbers: 45.70.-n, 05.65.+b, 81.05.Rm, 47.27.-i

I. INTRODUCTION

Granular gases are fascinating systems from the viewpoint of extending classical equilibrium statistical physics [1, 2]. To understand the fundamental mechanism of macroscopic properties between molecular gas (or liquid) and granular gas is one of the most important issues. Since granular motion is strongly affected by the energy source in general, the simple inelastic hard sphere (IHS) model without gravity, called the "freely evolving granular gas", has been much investigated. Those studies were investigated by using various methods based on several different levels, which are the microscopic (molecular dynamics (MD)) [3–8], the mesoscopic (*e.g.* Enskog-Boltzmann equation) [9, 10] and the macroscopic (Navier-Stokes (NS) equations, Ginzburg-Landau theory) [11–14].

To investigate on the macroscopic characters of the dissipative structure and the universal law, the analogies between granular system and fluid turbulence have been pointed out by several authors [15–17]. However, there are very few studies related to turbulence, because the dissipation mechanism of viscosity in the NS equation might be considered as completely different from that of inelastic collisions. First, Taguchi found numerically that the energy spectra from particle displacements at mid-depth in a 2D vibrated granular bed, which was composed of a few hundred particles, have a $-5/3$ exponent, similar to Kolmogorov scaling in 3D turbulence [15]. Then, neglecting the influence of gravity, a 2D granular gas with a Langevin-type thermostat was studied by Peng and Ohta in a system with about 10^3 particles [16]. Radjai and Roux [17] reported the spatial power-law spectrum of the particle displacements, as in Taguchi's work, in the quasi-static motions of the dense granular flow with a Parrinello-Rahman type boundary in a 2D MD model. All studies were performed in 2D and showed the power-law scaling of the energy spectrum and some relationship to NS turbulence. However, the special features of 2D NS turbulence were not shown.

In the inviscid limit of two-dimensional (2D) incompressible NS turbulence (*i.e.*, the Euler equation at high Reynolds number), energy and enstrophy are conserved in time. The enstrophy Z in 2D is defined by $Z = \frac{1}{2}\langle(\nabla \times \mathbf{u})^2\rangle$, where $(\nabla \times \mathbf{u})$ and $\mathbf{u} = (u_x, u_y)$ are the vorticity and the velocity, respectively. As a result, the most prominent dynamic features of 2D turbulence are two fluxes in the k-space. In the freely decaying turbulence, based on the dimensional analysis, a -3 power law in energy spectrum is derived under the assumption that the energy spectrum only depends on the enstrophy flux and the wave number (Kraichnan-Leith-Bachelor (KLB) Theory),

$$E(k) = C'\eta^{2/3}k^{-3}, \tag{1}$$

where C' is the Kraichnan-Batchelor constant and η is the enstrophy transfer rate [18, 19]. These cascade mechanisms are also much investigated by the direct numerical simulation (DNS) of NS equations. However, NS equation was constructed based on the phenomenological consideration, the results are highly nontrivial and difficult to understand especially at the microscopic molecular level.

In our previous study [20], we have investigated the macroscopic statistical properties on the freely evolving quasi-elastic IHS model by performing a large-scale event-driven molecular dynamics with mainly 512^2 particles system and found that remarkably analogous to an enstrophy cascade process in the freely decaying two-dimensional fluid turbulence. We found that there are four typical stages in the freely evolving inelastic hard disk system, which are homogeneous, shearing (vortex), clustering and final state. In the shearing stage, the self-organized macroscopic coherent vortices become dominant. In the clustering stage, the energy spectra are close to the expectation of KLB theory and the squared

*Electronic address: isobe@nitech.ac.jp

two-particle separation strictly obeys Richardson law. In this paper, to confirm the universal characters on the statistical laws of turbulence and investigate relationship between macroscopic patterns and microscopic dissipative origin, we have performed the simulation with 4096^2 particles system, which is 64 times larger than that of our previous works. We have reproduced the previous study with a clear quantitative evidence of the enstrophy cascade. To support the existence of a strong similarity between 2D IHS model and 2D NS fluid turbulence, we performed the extensive long-time simulations up to the final condensed states (attractor patterns) at the highly packing fraction in long time limit, in which a condensed state resembling Bose-Einstein condensation in 2D decaying NS turbulence [19]. Furthermore, to compare with the DNS of fluid turbulence quantitatively, we discuss the Reynolds number based on 2D Taylor microscale in our simulation.

II. MODEL AND NUMERICAL SETTING

The freely decaying 2D IHS model is so simple that the system is completely characterized by only three parameters: the restitution coefficient r, the total number of disks N, and the packing fraction ν. The system size L in units of disk diameter σ is $L/\sigma = \sqrt{\pi N/\nu}/2$. All disks are identical, so the system is mono-dispersive. For the dissipation, the normal restitution coefficient r for binary instantaneous collision is introduced (*i.e.*, parallel to the relative position of the two colliding disks in contact). Even in the quasi-elastic thermodynamic limit, the system becomes unstable and several spatio-temporal scales appear. The standard evolution scenario is that spatial instabilities occur from the initial homogeneous cooling state (HCS: 1st stage) to the velocity field (shearing regime: 2nd stage), and then to the density field (clustering regime: 3rd stage). Finally, global structures in the system (final attractor regime: 4th stage) appear as a non-equilibrium steady state, or local inelastic collapse occurs.

The system consists of up to about 16.8 million hard disks placed in a square box with periodic boundaries without any external force. To perform a large scale simulation, a simple and efficient event-driven algorithm is used [21]. Initially, the system is prepared in the equilibrium state (*i.e.*, the density is uniform and the disk velocities are Maxwell-Boltzmann distributed) by a long preparation run in an elastic system (*i.e.*, $r = 1$; the so-called the Alder solid-fluid transition occurs when the packing fraction is $\nu \sim 0.70$).

Because the total energy is monotonically decreasing in a freely evolving process, constant energy in time can be realized by attaching a thermostat. There are several types of thermostats to keep the total kinetic energy constant, roughly categorized as deterministic or stochastic. The advantage of a deterministic thermostat is that the trajectory of particles does not change compared with the non-thermostat case. Here, we introduce the new-scaled time t_s, which is described by $t_s = \int_0^t \beta(t)^{-1} dt$, $\beta(t) = \sqrt{T(0)/T(t)}$, where $T(t)$ is the average kinetic energy per particle as a function of the usual time t. Introducing a new-scaled time t_s instead of t is completely equivalent to adding a deterministic thermostat to the hard sphere system [22, 23]. Note that although the present system is attached with the so-called velocity scaling "thermostat", which is often used in the equilibrium system, it is known that the choice of thermostats affect the behavior of the granular system. In the previous studies, the IHS model with the Langevin thermostat [16] or multiplicative driving [24] are investigated, which might correspond to the situation in the forced turbulence. In the forced turbulence, the double cascade for both energy and enstrophy occurs, at which those exponents are $-5/3$ and -3, respectively. In the previous study such as Taguchi's work [15], the system is driven by vibrated beds, which might occurs energy cascade even for 2D. This might be considered that the spectrum show $-5/3$ exponent (resembling as Kolmogorov scaling) in 2D vibrated beds.

III. RESULTS

A. Energy Spectra

In Fig. 1, the typical evolution process of the energy spectra (power spectra of the "*kinetic temperature*" field, which are discretized by grids of size the disk diameter σ) at $(N, \nu) = (4096^2, 0.60)$ with respect to the nondimensional wave number divided by the energy dissipation for inelastic collisions $\sqrt{1-r^2}$ are shown. Because the local

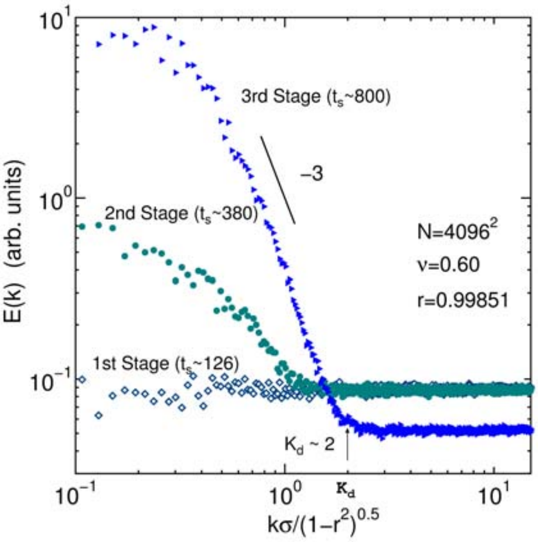

FIG. 1: Evolution of the energy spectrum. The exponent develops a maximum close to -3 during the 3rd stage, during which the enstrophy dissipation finishs. The parameters are set at (r, N, ν)=$(0.99851, 4096^2, 0.60)$.

equilibrium assumption in a granular system is not valid, we regard the granular temperature as the "*kinetic temperature*" only in the almost elastic case ($r \sim 1$). Our large-scale simulations show that $E(k)$ develops towards an exponent -3 for small wavenumbers (large scale), until the onset of the clustering regime (3rd stage) [20], as is expected by the KLB theory for freely decaying 2D NS fluid turbulence. In Fig. 1, we can also estimate the characteristic spatial scale K_d $(= k\sigma/\sqrt{1-r^2}) \sim 2$ as the minimal dissipative domain, which is composed of about $\sim 10^3$ disks. During the evolution of $E(k)$ for small wavenumbers, the minimal dissipation scale K_d appears not to change.

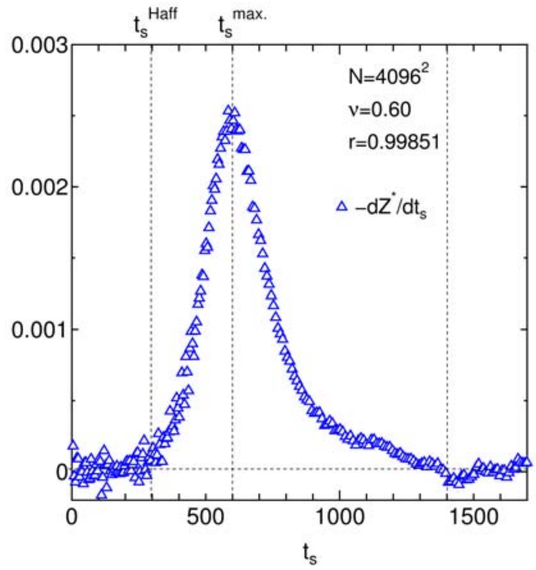

FIG. 2: Evolution of the dissipation rate of the enstrophy $-dZ^*/dt_s$ in the unit of scaled time t_s is shown. It reaches a maximum at the onset of the clustering instability. The parameters are set at (r, N, ν)=$(0.99851, 4096^2, 0.60)$.

In Fig. 2, the typical time evolution of the dissipation rate for enstrophy $-dZ^*/dt_s$ are shown, where property Z^* are estimated in units of scaled time t_s. We found that the peak of enstrophy dissipation take a maximum around the boundary time between the shearing regime (2nd stage) and the clustering regime (3rd stage). Therefore, the enstrophy dissipation rate provide a criterion to determine the time between the shearing and clustering regimes. The enstrophy dissipation is almost finished around $t_s \sim 1400$, at which time the exponent of the energy spectrum reaches a maximum. We found that the relationship between the enstrophy cascade in energy spectrum (Fig. 1) and the time evolution of the enstrophy dissipation rate (Fig. 2) behaves consistent with each other.

Developing turbulent patterns in the vorticity fields around onset of clustering regime ($t_s \sim 500$(left)) and fully developed regime ($t_s \sim 1000$ (right)) are shown in Fig. 3. We confirmed that the self-organized vortices gradually increase, which is resembling to the fully developed turbulence in DNS of the decaying process of NS equation. In the fully developed regime, typical density and temperature fields around $t_s \sim 1000$ in clustering regime (3rd state) are also shown in Fig. 4, in which the parameter are the same as Figs. 1 and 2. In the left of Fig. 4, the highly dense packing inhomogeneous clusters are observed in the system, however, they behave dynamically where the string-shape clusters are actively moving (i.e. like fluids) and are colliding with each other. The spatial fourier transform of the temperature fields (the right of Fig. 4) correspond to the energy spectra. We found that the almost regions of the higher temperature appear around the edge of string-like clusters where the particles flow collectively. Based on these figures, the system is fully fluidized and recognized as "far from (quasi-)solid" (i.e., diffusion constant is relatively high.). In such a case, the dynamical turbulent behavior might not be much affected by the polydispersity (crystallization effects).

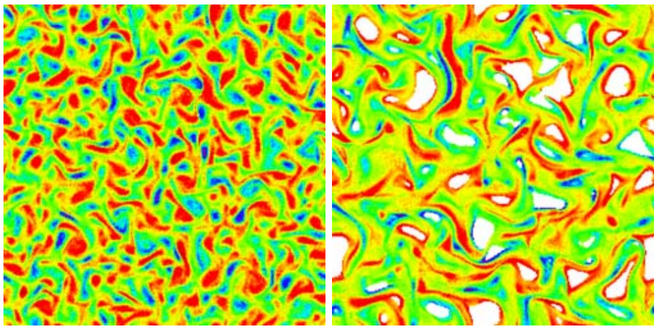

FIG. 3: Developing turbulent patterns in the vorticity fields around $t_s \sim 500$(left) and ~ 1000 (right). The parameters are the same as in Figs. 1 and 2.

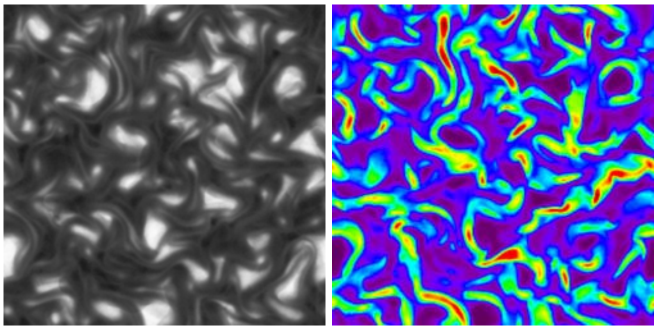

FIG. 4: Developed turbulent patterns in the density (left) and temperature (right) fields around $t_s \sim 1000$. The parameters are the same as in Fig. 3.

B. Microscale Reynolds Number

In the fluid turbulence, the quantitative properties are characterized by Reynolds number. Here, we estimate the Reynolds number in granular gas. The Taylor microscale λ in homogeneous isotropic incompressible 2D NS turbulence with zero mean velocity can be derived as $\lambda = \sqrt{8\nu_{\rm vis}\left\langle u_x^2\right\rangle / \langle\epsilon\rangle}$, where $\nu_{\rm vis}$ and $\langle\epsilon\rangle$ are the kinematic viscosity and the energy dissipation rate, respectively. For a hard disk fluid, the kinematic viscosity $\nu_{\rm vis} = \eta_E/\rho$ can be derived by the density $\rho(= mn)$ and Enskog shear viscosity η_E, which is given by the Enskog theory for 2D hard disk systems [25],

$$\eta_E = \eta_0\gamma\rho\left\{\frac{1}{\gamma\rho\chi} + 1 + \gamma\rho\chi\left(\frac{1}{4} + \frac{2}{\pi\gamma_0(3)}\right)\right\}, \qquad (2)$$

where $\eta_0 = (\gamma_0(3)/2\sigma)\sqrt{mkT/\pi}$, $\gamma\rho = \pi\sigma^2 n/2 = 2y$, $\chi = (1-7y/16)/(1-y)^2$(Enskog scaling factor), $y = \pi\sigma^2 n/4$, and n is number density. Here we use in the third Sonine polynomial approximation $\gamma_0(3) = 1.022$.

The Reynolds number based on Taylor microscale $\lambda(t_s)$ can be estimated as,

$$R_\lambda(t_s) = \frac{\left\langle u_x^2\right\rangle^{\frac{1}{2}}\lambda(t_s)}{\nu_{\rm vis}}. \qquad (3)$$

Because we can estimate the energy dissipation rate per unit mass $\langle\epsilon\rangle = -d\mathcal{E}/dt_s$ via Haff's law and the kinematic viscosity via Enskog theory, we can roughly estimate $R_\lambda \sim 19.2$ at $t_s = 0$. However, R_λ increases to 286.2 around $t_s \sim t_s^{\rm Haff}(\sim 300)$ at the onset of the deviation from Haff's law in the kinetic energy decaying functions. Although the granular gas system is well described as the compressible macroscopic fluid equations, we can regard that the system is still almost homogeneous in the early stage of relaxation. Therefore, before the clustering regime begins ($i.e.$, $t_s < t_s^{\rm Haff}$), the derivation of Taylor's microscale expression Eq. (3) may be considered valid. This assumption is also confirmed to be fairly good approximation by the calculation of the fluctuation of density as shown in the Fig. 1 of Ref. [20].

C. Final Condensed States

Granular clustering as a result of a hydrodynamic instability without gravity has been investigated by many authors [2]. A hydrodynamic equation to describe both the clustering stage and the final attractors in a granular gas (IHS model) has been proposed [26–28]. In this theory, an additional term to calculate the effective pressure due to the excluded volume effect was introduced phenomenologically. This treatment avoids inelastic collapse and leads to an efficient direct numerical simulation (DNS), even in dense systems. By systematic calculations, these studies found three final attractors: the homogeneous cooling state (HCS), the shear band state (SBS), and the two-vortex state (2VS). The authors mentioned that there was no clear criterion between SBS and 2VS, which were dependent on slight differences in their initial conditions. The existence of a 2VS mode has already been pointed out for dense systems [29].

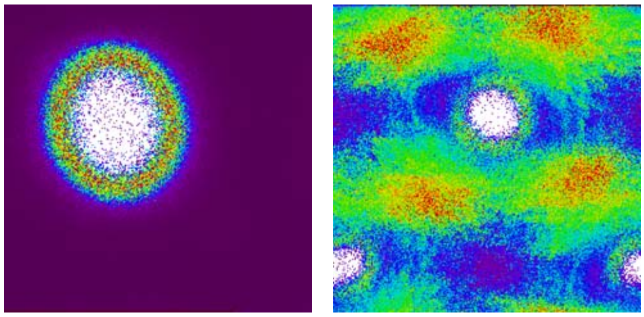

FIG. 5: Temperature fields for the final attractors in high packing systems ($\nu = 0.75$, $N = 512^2$). The restitution coefficients are $r = 0.9968$ (left) and $r = 0.9953$ (right), respectively. We found that one or two voids were present in the density, which are surrounded by closely packed solids.

A phenomenological amplitude equation was discussed analytically for the above two modes (SBS or 2VS) [23]. In the dense system, we found not only SBS and 2VS, but also another final attractor by systematic runs in the quasi-elastic limit. This had only one void in the density field, which we called it the one-vortex state (1VS). In Fig. 5, the typical cases of 1VS (left) and 2VS (right) at $\nu = 0.75$ in the *kinetic temperature* field are shown, which are evolved to the final states after ~ 9000 collisions per particle in $N = 512^2$ system. There is one void in the density, which is surrounded by the "close packing" solid at $\nu \sim 0.90$. Only particles near the edge of the void-crystal boundaries are moving actively. It therefore looks like a ring shape in the *kinetic temperature* field. The prediction of final attractors seems to be difficult, because different final attractors (1VS and 2VS) appear even if the restitution coefficient is almost the same. As the previous studies based on hydrodynamic equations pointed out, we expected that there are no clear criterion between those attractors, which are just dependent on slight differences in their initial conditions. In case of 1VS, we found close packing fraction around the void. Therefore, the polydispersity will be expected to be much influence on the shape of attractors. These results are outside expectations of the previous phenomenological theory. In dense systems, other physical mechanisms might be relevant, such as the condensed state in terms of the 2D turbulence. Indeed, in the study of 2D turbulence, when the correlation scale ($e.g.$, the two-particle dispersion) becomes larger than the boundary (system) size, the energy cascade to lower k condenses in the lowest mode, and the one- or two- vortex states appear. A type of "Bose-Einstein condensation" in a finite box was pointed out by Kraichnan [19] and numerically discovered in the

DNS calculation by Smith & Yakhot [30]. From this point of view, it is interesting to study the relationship between granular gases and Bose-Einstein condensation.

D. Minimal Dissipative Scale

We, then, focused on the minimal wavenumber of spatial correlations K_d in the temperature field. As predicted by kinetic theory, the values of the minimal wavenumber K_d can be scaled with a function of the restitution coefficient $\sqrt{1-r^2}$. Figure 6 shows various values of $E(k)$ at the onset of clustering regime, scaled by a function of the restitution coefficient over a wide parameter space when the packing fraction is fixed at $\nu = 0.60$ in $N = 4096^2$ system. Even when the systems have already evolved to the beginning of the clustering instability, the scaling behavior for the minimal dissipation is valid.

The minimal scale for dissipation l_d in the enstrophy cascade is also theoretically estimated by using ν_{vis} and η as,

$$\frac{l_d}{\sigma} = \left(\frac{\nu_{\text{vis}}^3}{\eta}\right)^{-\frac{1}{6}}. \quad (4)$$

Based on about estimation of l_d/σ above equation, it decreases toward ~ 26 around $t_s \sim t_s^{\max}$, in which the minimal dissipation scale of wave number increases up to $K_d \sim 0.9$ during evolving process due to the growth of enstrophy dissipation rate (see, Fig. 2). On the other hand, we found that the estimations of the wavenumber length of minimal dissipation are $K_d \sim 2$ in the energy spectra (Fig. 6). Since the clustering regime gradually starts around $t_s \sim t_s^{\max}$ and some ambiguities of estimation related to the minimal scale, it is proved that the minimal length obtained by both analyses are of same order. We conclude that there are close relationships of the minimal scale for dissipation between the equation derived by enstrophy cascade and the length of minimal dissipation estimated in the energy spectra. Figure 6 shows that the inertial range grows gradually when the restitution coefficient is close to unity. This suggests that the Reynolds number becomes higher in the quasi-elastic limit, which is also resembling a fluid of Euler equation at high Reynolds number in the inviscid limit.

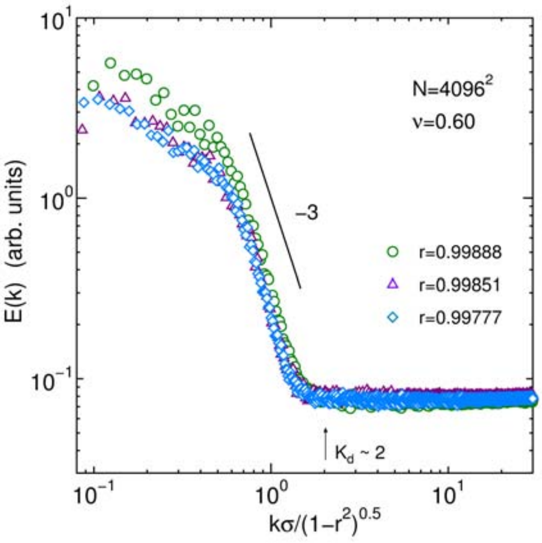

FIG. 6: Scaling behavior of the energy spectra at the onset of the clustering regime for different restitution coefficients r at a fixed $(N, \nu) = (4096^2, 0.60)$.

IV. CONCLUDING REMARKS

In this paper, we showed several features of 2D NS turbulence in granular gases using the well-defined simple IHS model. By extensive event-driven molecular dynamics and systematic estimations of the spatial correlation in a wide parameter space, two typical features of 2D NS turbulence (*i.e.*, the enstrophy cascade and the Bose-Einstein condensation) were found in the relatively dilute (fluid-like) early stages and dense (solid-like) final stages of the granular gas, respectively. We also found that the relationship between the enstrophy cascade in energy spectrum and the time evolution of the enstrophy dissipation rate is consistent with each other and the enstrophy dissipation rate provide a criterion to determine the time between the shearing and clustering regimes. The exponent of energy spectra were the developed to the same as expected from KLB theory after the enstrophy dissipation finished in the clustering stage. The minimal dissipation scale depended on the restitution coefficient and could be scaled by a function of the restitution coefficient. In the quasi-elastic limit, because the features of turbulence clearly appear, the system has a high Reynolds number $R_\lambda \sim 286.2$ in our simulation. In general, because the laboratory and industrial turbulent flows are characterized by $R_\lambda \sim \mathcal{O}(10^2 \sim 10^3)$, it is quite reasonable that the granular gas system shows the specific laws of turbulent behavior. Previous studies [15–17] cannot show these features. The main possible reasons for this are summarized as the following: (a) the statistical errors are quite large because of the small number of particles, (b) the system size is too small and is comparable to the minimal spatial correlation lengths (such as the Kolmogorov dissipative length), (c) no systematic parameter surveys exists, and (d) the unique features of 2D turbulence are not well-known in the granular physics community. Our results suggest that the granular gas in the quasi-elastic and thermodynamic limit is strongly related to 2D NS turbulence.

Acknowledgments

I would like to thank to T. Watanabe and J. Wakou for helpful comments. This study was supported by Grant-in-Aid for Scientific Research from the Ministry of Education, Culture, Sports, Science and Technology No. 23740293. Part of the computations was performed using the facilities of the Supercomputer Center, ISSP (Univ. of Tokyo), RCCS (Okazaki), Japan. This work is also performed with the support and under the auspices of the NIFS Collaboration Research program (NIFS11KNTS010, NIFS11KNSS020).

[1] L. P. Kadanoff, *Rev. Mod. Phys.* **71**, 435 (1999).
[2] I. Goldhirsch, *Annu. Rev. Fluid Mech.* **35**, 267 (2003).
[3] T. Pöschel and T. Schwager, *Computational Granular Dynamics* (Springer, 2004).
[4] S. Chen, Y. Deng, X. Nie and Y. Tu, *Phys. Lett. A* **269**, 218 (2000).
[5] S. Miller and S. Luding, *Phys. Rev. E* **69**, 031305 (2004).
[6] X. Nie, E. Ben-Naim and S. Chen, *Phys. Rev. Lett.* **89**, 204301 (2002).
[7] B. Meerson and A. Puglisi, *Europhys. Lett.* **70**, 478 (2005).
[8] J. I. Alvarez-Hamelin and A. Puglisi, *Phys. Rev. E* **75**, 051302 (2007).
[9] N. Brilliantov and T. Pöschel, *Kinetic Theory of Granular Gases* (Oxford University Press, 2004).
[10] J. J. Brey, J. W. Dufty and A. Santos, *J. Stat. Phys.* **87**, 1051 (1997).
[11] T. P. C. van Noije, M. H. Ernst, R. Brito and J. A. G. Orza, *Phys. Rev. Lett.* **79**, 411 (1997).
[12] J. Wakou, R. Brito and M. H. Ernst, *J. Stat. Phys.* **107**, 3 (2002).
[13] E. Efrati, E. Livne and B. Meerson, *Phys. Rev. Lett.* **94**, 088001 (2005).
[14] B. Meerson, I. Fouxon and A. Vilenkin, *Phys. Rev. E* **77**, 021307 (2008).
[15] Y. -H. Taguchi, *Europhys. Lett.* **24**, 203 (1993).
[16] G. Peng and T. Ohta, *Phys. Rev. E* **58**, 4737 (1998).
[17] F. Radjai and S. Roux, *Phys. Rev. Lett.* **89**, 064302 (2002).
[18] R. H. Kraichnan and D. Montgomery, *Rep. Prog. Phys.* **43**, 547 (1980).
[19] P. Tabeling, *Phys. Rep.* **362**, 1 (2002).
[20] M. Isobe, *Phys. Rev. E* **68**, 040301(R) (2003).
[21] M. Isobe, *Int. J. Mod. Phys. C* **10**, 1281 (1999).
[22] T. S. Komatsu, *J. Phys. Soc. Jpn.* **69**, 5 (2000).
[23] R. Soto, M. Mareschal and M. Malek Monsour, *Phys. Rev. E* **62**, 3836 (2000).
[24] R. Cafiero, S. Luding and H. J. Herrmann, *Phys. Rev. Lett.* **84**, 6014 (2000).
[25] D. M. Gass, *J. Chem. Phys.* **54**, 1898 (1971).
[26] S. A. Hill and G. F. Mazenko, *Phys. Rev. E* **63**, 031303 (2001).
[27] S. A. Hill and G. F. Mazenko, *Phys. Rev. E* **67**, 061302 (2003).
[28] S. Marakani and G. F. Mazenko, *cond-mat/0406572*.
[29] S. McNamara and W. R. Young, *Phys. Rev. E* **53**, 5089 (1996).
[30] L. M. Smith and V. Yakhot, *Phys. Rev. Lett.* **71**, 352 (1993).